PNAS
www.pnas.org

Supplementary Information for

Lipofuscin causes atypical necroptosis through lysosomal membrane permeabilization

Chendong Pan, Kalpita Banerjee, Guillermo L. Lehmann, Dena Almeida, Katherine A. Hajjar, Ignacio Benedicto, Zhichun Jiang, Roxana A. Radu, David H. Thompson, Enrique Rodriguez-Boulan and Marcelo M. Nociari[#].

Email: mnociari@med.cornell.edu

This PDF file includes:

Supplementary MATERIALS & METHODS

Study design. The objective of our study was to identify novel interventional approaches for protecting against lipofuscin buildups.

Differentiation of ARPE-19 and hfRPE cells. To grow fully confluent monolayers of polarized ARPE19 cells, $2x10^5$ cells were seeded per transwell insert (12 mm diameter, 0.4 µm pore; polystyrene, Corning) in 1% DMEM medium for at least 4 weeks before further experimentation. hfRPE cells from donors at 16 to 18 weeks' gestation were kindly provided by Sheldon S. Miller and A. Maminishkis (National Eye Institute, NIH). Newly received batches of cells were first expanded on 6 well plates with RPE medium (15% FBS, 1% penicillin/streptomycin and supplements in MEM-α modified medium) for 3 weeks, at 37 ºC, 5% CO_2. hfRPE were used in passage 1. Differentiation of hfRPE cells was done following Maminishkis' et al. protocol (78). Briefly, cells were seeded in the 12 mm transwells (Corning) with 5% RPE medium for 3 days to ensure total confluency, media was then switched to 1% FBS RPE medium with 10 µM ROCK kinase inhibitor (Y-27632 (Tocris)), for one week. Thereafter, cells were maintained in 1% FBS RPE medium, without ROCK inhibitor for more 3 weeks, with two changes per week, before evaluation of polarity and differentiation markers.

Cell Viability Assays. 80% confluent cells (seeded 2 days earlier), in 96 well plates, were pre-treated either 1hr or overnight, with inhibitors or antioxidants, respectively (TABLE. S1), followed by incubation with A2E/ATRD or vehicle (ethanol control) in serum free OptiMEM medium and for additional 24 h at 37 ºC. End-point cell viability was assessed using Resazurin fluorescence (555 nm ex/ 585 nm em), in a microplate-fluorescence reader (SpectraMax M5e, Molecular Devices, CA, USA), or using NucView405/DRAQ7 mix for real time monitoring of cell-death in an automated confocal fluorescence microscope. For real-time cell death, 2μM NUCView 405 (Biotium, cat.no.10407) and 0.6 μM of DRAQ7 were added per well, of a glass bottom 96 well plate (μ-Plate 96 Well Black, ibidi), and the fluorescence signals were monitored every 30 min according to manufacturers' instructions. The exact timing of appearance of far-red (DRAQ7 = plasma membrane leakage) and blue (NUC405 = caspase 3 activation) fluorescence signals were critical to differentiate apoptosis and necrosis from secondary events, such as membrane damage and generalized proteolytic activation during the late phase of apoptosis and necrosis, respectively. For blue-light induced apoptosis, A2E/ATRD or vehicle loaded cells were placed in HBSS and exposed 15 min to a 90-Watt high power LED light (cat#2506BU) with 430 ± 20 nm wavelength illumination. HBSS was then replaced by OptiMEM medium and this was considered the start time for monitoring cell death.

Animals. Pigmented ABCA4/RDH8 knockouts, RPE65-Leu450, were freed of crb1 mutation by in house backcrossing with C57BL6J, both from Jackson laboratories. Genotyping was performed at Transnetyx (Memphis, TN). Only mice with Abca4$^{-/-}$ Rdh8$^{-/-}$, Rpe65-Leu450 but no crb1 mutations (retinal degeneration slow) were maintained in the colony. Controls C57BL/6J (Rpe65-Leu450, crb1negative) were also Jackson's lab. All mice were housed at Weill Cornell Medicine's animal facility under a 12hr light (~10 lux) / 12hr dark cycle environment or under complete darkness. Experimental manipulations in the dark were done under dim red light transmitted through a Kodak No. 1 safelight filter (transmittance >560 nm). No retinal degeneration or necroptosis markers were appreciably detected in 20 months or older C57BL6/N (Rpe65-Met450, crb1 positive) obtained from the NAI/NIH. All animal procedures and experiments were approved by the Animal Care and Use Committee of Weill Cornell Medical College in agreement with the guidelines established by the NIH Office of Laboratory Animal Welfare and the Association of Research for Vision and Ophthalmology (ARVO) statement for the use of animals in ophthalmic research.

RPE and Neural retina flat mounts. Mouse eyes were enucleated and placed in 4% PFA dissolved in PBS for 1 h at room temperature. After fixing, a 23G needle was used to make a hole at the limbus area and iris scissors used to cut around the circumference of the limbus, remove the cornea, iris and lens, separate the neuronal retina and sclera with micro-forceps. Neuronal retina and RPE layer were dissected out and incubated with blocking buffer (1% BSA and 0.3% Triton-X-100 in PBS) for at least 20 min. Primary antibodies were added to the blocking buffer and kept at 4 ºC at least overnight. Retina and RPE layer were washed and incubated with secondary antibodies for at least 3 hrs at room temperature, then washed with PBS three times. Under the dissection microscope, retina or RPE layer was cut into a four-leaf clover shape and mounted on the slides using mounting medium (EMS glycerol mounting medium with DAPI and DABCO, cat. No. 17989-61). Slides were stored at 4 ºC until imaging.

Human Retinas.
De-identified sections or whole human eyes were received from the National Disease Research Institute (NDRI, Philadelphia) and from The Eye-Bank for Sight Restoration, Inc

(New York, NY), respectively. All AMD donors were diagnosed pre-mortem with either no-ocular pathology or non-neovascular (dry-AMD). The clinical diagnosis from the eyes received from NDRI was confirmed by histopathologic post-mortem examination. Eyes from the NDRI were processed within 10 hours of death. First, they were cryoprotected through graded sucrose to 20%, and further embedded into Tissue-Tek OCT (Sakura Finetek, Torrance, CA, USA). 8µm sections were cut at − 25 ◦C and mounted on glass microscope slides then shipped from NDRI on dry ice and stored at − 20 ◦C until immunohistochemistry was performed. The eyes received from The Eye-Bank were collected as whole eyes within 24hours of postmortem. The eyes were fixed in 4% paraformaldehyde for 24hrs. The cornea, lens and vitreous were removed and the eyes cryoprotected in 30% sucrose overnight. The eyes were embedded in 2 parts OCT/ 1 part 30% sucrose and sectioned at 8µm. Tissue sections from 8 donors (5 female and 3 male). ages ranged from 42 to 86 years. Four donors were considered “normal” with no history of retinal disease; however, one showed sporadic druse and abundant lipofuscin in the RPE and was later classified as early AMD. The other four donors had a history of dry-AMD. Slides requested from the NDRI were sections in the mid-periphery, in proximity to the macula and eyes received from the eye bank were sectioned at Weill Cornell Medicine.

Cryosections and staining. Mouse eyes were fixed with 4% PFA and embedded in 30% sucrose overnight at 4 ºC, then cryopreserved in Tissue-Tek OCT compound (Sakura Finetek, Torrance, CA, USA) and cut into 15µm sections. Sections were blocked with 1% BSA and 0.1% Triton X-100 PBS, and then immunofluorescence staining was performed using standard methods and the appropriate dilutions of primary antibodies (Table S2). Negative controls were included in each staining, and slides were mounted with anti-fade mount medium. Slides were stored at 4 ºC before analysis on a Zeiss SD microscope using Zen software. For paraffin sections, mouse eyes were fixed in 4% paraformaldehyde, 16.8% isopropyl alcohol, 2% trichloroacetic acid and 2% ZnCl2 in phosphate buffer and sent out to the pathology core for embedding and sectioning into 5-□m slices. Standard protocol was applied to deplete paraffin. Briefly, paraffin slides were put into Xylene for 2 min, twice; then in 100% ethanol for 2 min, and then 95% ethanol for 2 min. After deparaffinization slides were stained with either H&E or antibodies. For H&E slides were incubated in Hematoxylin for 3 min, followed by Eosin for 45 sec, then 95% ethanol for 1 min, and 100% ethanol for 1 min twice, before mounting. For immunostaining, slides were incubated in blocking buffer for 2 h, primary antibodies overnight at 4ºC followed by secondary fluorescent label antibodies for 2hr at room temperature. For de-myelinization, deparaffinized were immersed into PBS with 10% H2O2 at 55 ºC for 5 min and then immune-stained following standard procedure.

Intravitreal treatment. Under a surgery microscope, mouse eyes were placed in the center of the field and a 33 gauge of needle was inserted into the eye at the ora serrata and towards the ONH. Nec7 (2.0µL of 132mM stock in DMSO) were intravitreally injected in one eye and the companion eye received an equal amount of vehicle (DMSO). For p-MLKL staining, eyes were harvested after 1 week and were analyzed by immune-fluorescence and H&E. For long term experiments with Nec7, DKO mice were injected at 7 months old every other month for a total of 3 times.

Lipofuscin synthesis. A2E was synthesized and purified by HPLC (>97%) according to a published protocol (2). Quality of the material was assessed by MS and UV-absorbance between 250 and 600 nm to rule out contamination of all-trans retinal from the synthesis and oxidative degradation of the material.

HPLC analysis of bisretinoid content. Bisretinoids were extracted from mouse eyecups under red dim light. Briefly, single mouse eyecups (containing RPE/choroid/sclera, devoid of neural retina) washed with phosphate buffer (PBS) and homogenized in PBS. Chloroform/methanol (4 uL, 2:1, vol/vol) was added, and the samples were extracted with the addition of 4 mL chloroform and 3 mL dH_2O, followed by centrifugation at 1000 g for 10 min. Extraction was repeated with the addition of 4 mL chloroform. Organic phases were pooled, filtered, dried under a stream of argon, and redissolved in 100µL 2-propanol. Bisretinoid extracts were analyzed by normal-phase HPLC with a silica column (Zorbax-Sil 5µm, 250 × 4.6 mm; Agilent Technologies, Wilmington DE) as previously described (3). The mobile phase was hexane/2-propanol/ethanol/25mM potassium phosphate /glacial acetic acid (485:376:100:45:0.275 vol/vol) and was filtered before use. The flow rate was 1 mL/min. Column and solvent temperatures were maintained at 40 °C. Absorption units at 435 nm were converted to picomoles using a calibration curve with an authentic A2E standard and the published molar extinction coefficient for A2E; the identity of each bisretinoid peak was confirmed by online spectral analysis.

Immunoblotting. Total cell lysates were prepared in RIPA buffer (50 mM TrisHCl, pH 8.0, 150 mM NaCl, 1% NP40, 0.5% Sodium Deoxycholate, 0.1% SDS, protease-phosphatase inhibitors (Thermo Scientific, cat# A32962)). Lysates were sonicated for 40 sec followed by centrifugation at 12,000g for 10 min. Protein concentration in homogenates were assessed by Pierce Rapid Gold BCA protein assay (ThermoFisher, cat. # A53225); 30 µg of protein were loaded per lane of 10 wells 4-12% Nupage gels (ThermoFisher, cat. # NP0336BOX), separated at 100 V for 2 h and transferred into wet nitrocellulose membranes (Whatman, PROTAN BA83) overnight at 20 V. Membranes were blocked with 5% milk in TBS for 2 h and then primary antibodies were added in Tris Buffered Saline 0.1% Tween-20 (TBS-T) overnight at 4 °C. The next day, the membranes were washed and incubated for 2 h at room temperature with horse radish peroxidase-conjugated secondary antibody (cat # G21234, Invitrogen) at a 1:10,000 dilution. After 3 more washes, membranes were probed with enhanced chemiluminescence (ECL) reagent and detected using X-ray films for chemiluminescence images (GE healthcare, RPN2106). Antibodies for Western blotting are listed in Table. S2. Scanning/imaging and quantitation of the image was done using SilverFast 8 application software and Fiji Image J.

Quantification of Outer Nuclear Layer (ONL) thickness. Thickness of outer nuclear layers were quantified in paraffin embedded, H&E counterstained cross sectioned retinas. A light microscope was used to capture digital images that were stitched by the software. ONL thickness was measured at 0.1 mm intervals superior and inferior to the edge of the optic nerve head along the vertical meridian. The center of the ONH was used as the start of the measurement. The thickness of ONL was measured by Zen software.

Quantification of RPE nuclei. RPE nuclei were quantified in paraffin embedded, H&E counterstained cross sectioned eyes. Images were taken at 40x and stitched by the Zen software. The number of RPE nuclei were counted at every 0.1mm interval and plotted as a function of distance from ONH in 23-month-old DKO (n = 10) and 27-month-old WT mouse retinas (n = 8). Mean values (±SEM) were significantly different at each point ($p<0.05$).

Quantification of RPE cell size. RPE eyecups were dissected out of mouse eyes, stained with Alexa647-phalloidin, for 1 h at room temperature and flat-mounted, to visualize autofluorescence and cell borders. Fluorescent images were acquired with a Zeiss Spinning Disk confocal microscope using a 63x objective. RPE layers were imaged

from the optic nerve head to the periphery. The areas of individual RPE cells were measured using ImageJ.

Cathepsin activity assay. 50,000 cells were seeded per well in 96 well plate. Cells were treated with A2E or LLOMe in presence or not of inhibitors (arimoclomol or nec7). After 5 min incubation, media were replaced with 75ul 100mM phosphate buffer, pH6 and permeabilized with either digitonin 30ug/ml (for plasma membrane only); or 150ug/ml (for plasma membrane and lysosome membranes) on ice for 10 min with slow shaking. 25ul of reaction substrate solution containing 5mM DTT+50uM Z-FR-AMC (R&D systems, cat#ES009) +50uM MCA-GKPILFFRL(Lys (DNP))r-NH2(echelon-inc, cat# 839730-93-7) were added and kept in dark for 20min, 25ul of stop solution (2M Na2CO3, 1M glycine) were then added followed by the measurement of cleaved AMC by fluorescence (ex/em 370/460).

Statistics. All data were processed in Prism7.0 software. ANOVA, Student's t test or multiple t test was used when appropriate. P values less than 0.05 were considered statistically significant.

Figures S1 to S6

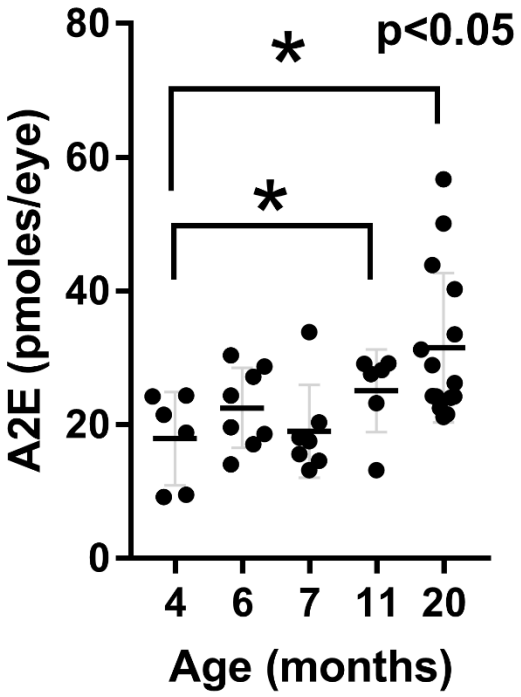

Fig. S1. HPLC quantitation of the content of A2E in the RPE of DKO mice at the ages indicated (mean ±SD, $p<0.05$). Each dot corresponds to one eye.

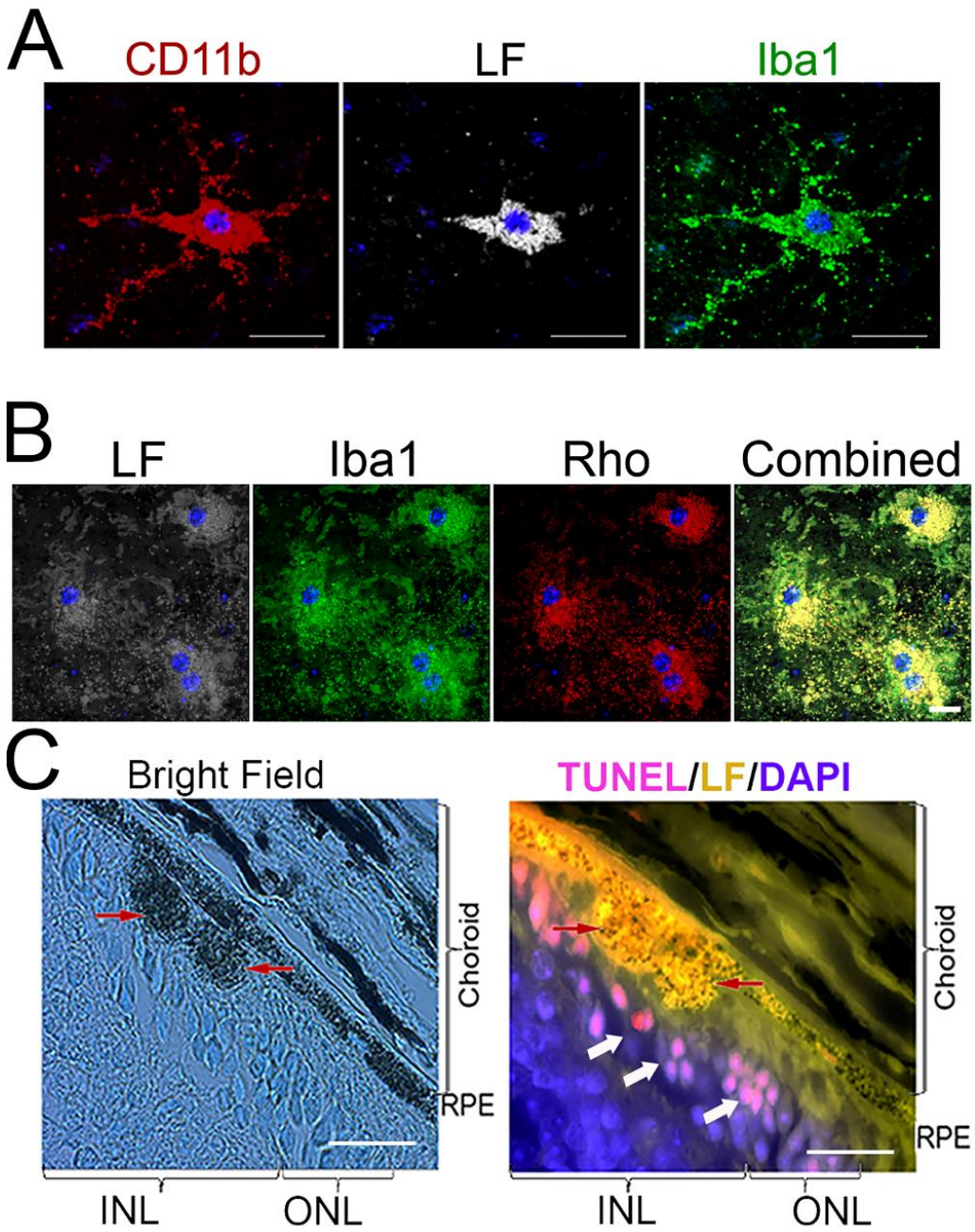

Fig. S2. Additional degenerative changes in retinas with lipofuscin buildup. (A) Infiltrated cells detected in RPE flat mounts from 23-months-old DKO, but not WT mice. These cells were CD11b+ (red), Iba1+ (green) and lipofuscin+ (white) (63X magnification). Scale bars are 20 μm. (B) Iba1+ infiltrated cells detected in RPE flat mounts from 18 months old DKO contain lipofuscin and rhodopsin. Scale bar is 10 μm. (C) Left bright field image with two melanin positive RPE cells ~10 μm fragments (red arrows) shed into the neural retina. Right image shows generalized photoreceptor cell-death (white arrows, TUNEL positive) in the zones contiguous to the shedding RPE which depict higher levels of lipofuscin than RPE neighbors. Bars are 20 μm.

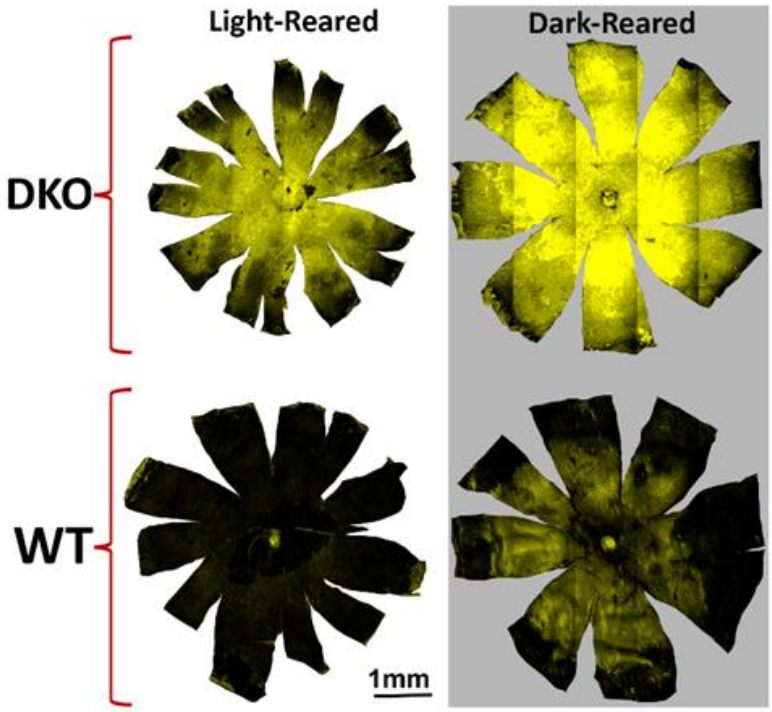

Fig. S3. Higher content of lipofuscin in the RPE of dark reared animals. Autofluorescence of RPE eyecups (in yellow) was used to estimate the amount of lipofuscin in 12 months old DKO and WT mice raised in the dark or under 12 h light cycles. Low magnification (10X) images were stitched together from individual fields, to reconstitute lipofuscin content of the entire back of the eyes. Dorsal–top; ventral–bottom; nasal–right; temporal–left. Scale bar = 1 mm.

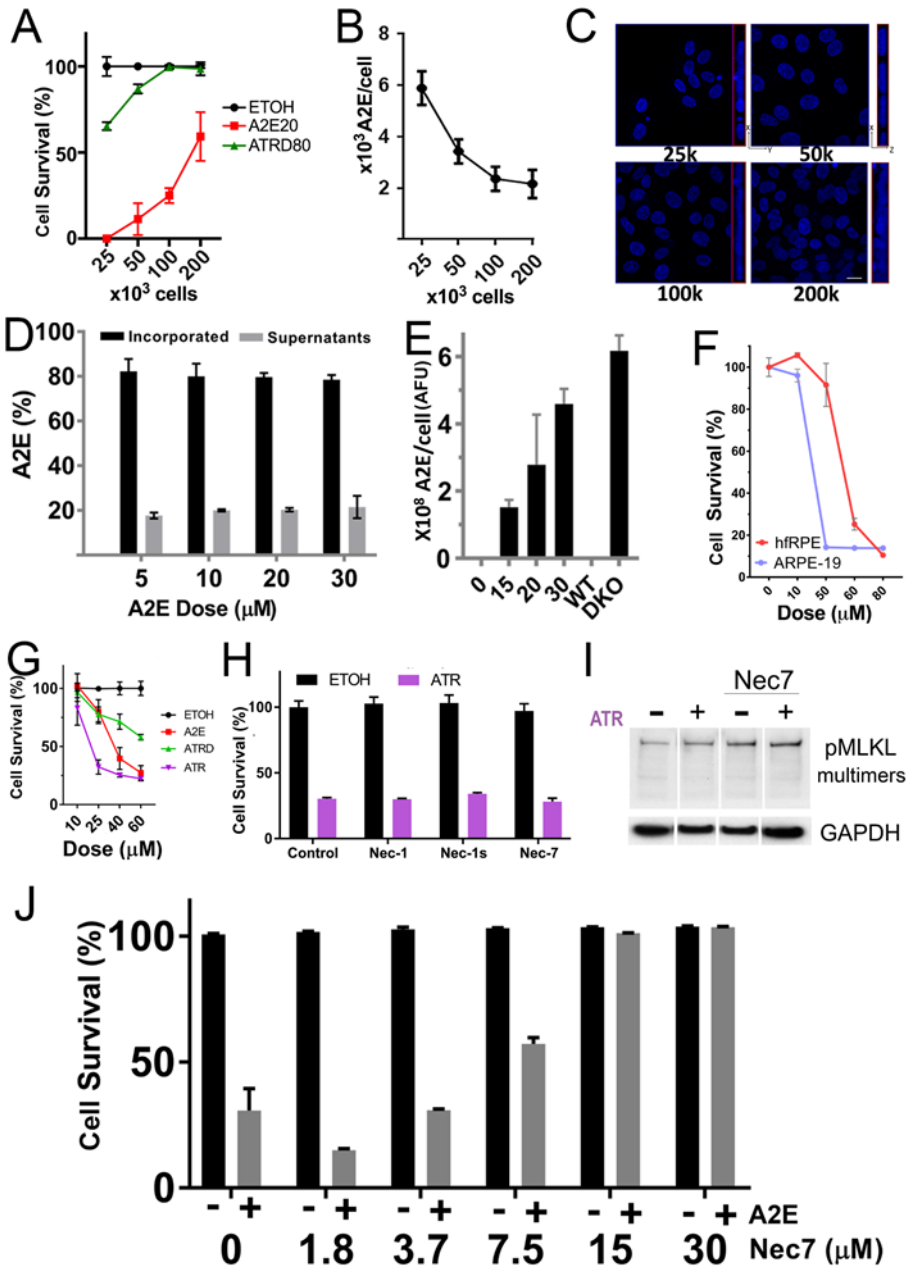

Fig. S4. Cell-death assay to study light-independent lipofuscin cytotoxicity. (A) 24 h cytotoxicity of A2E (20 μM) and ATRD (80 μM) in ARPE-19 cell cultures was affected by cell confluency. (B) Increased cell confluency reduced the amount of A2E uptaken into cells. (C) Maximal projected images of Hoechst stained ARPE19 cultures at confluences used in (B) to confirm they grew in monolayers. Scale bar=10 μm. (D) Different A2E doses incorporated with equal (80%) efficiency in 80% confluent cultures (n=3, mean±SEM). (E) Lipofuscin/cell incorporated *in vitro* during cytotoxicity assays were in the same range found in RPE cells from 1year old DKO retinas. (F) Light-independent lipofuscin cell-death in ARPE19 (blue) and hfRPE (red). (G) Light-independent cytotoxicity of A2E, ATRD, and ATR in ARPE19. (H) Nec1, Nec1s, or Nec7 did not protect against ATR ($p<0.001$, n=4, mean±SEM, paired t test). (I) Western blot showing that MLKL is not phosphorylated upon ATR ± Nec7 treatments. (J) Dose dependent Nec7 protection against 15μM A2E dark cytotoxicity in ARPE19 cells. ($p<0.001$, n=3, mean±SEM, paired t test, GraphPad Prism 7.0).

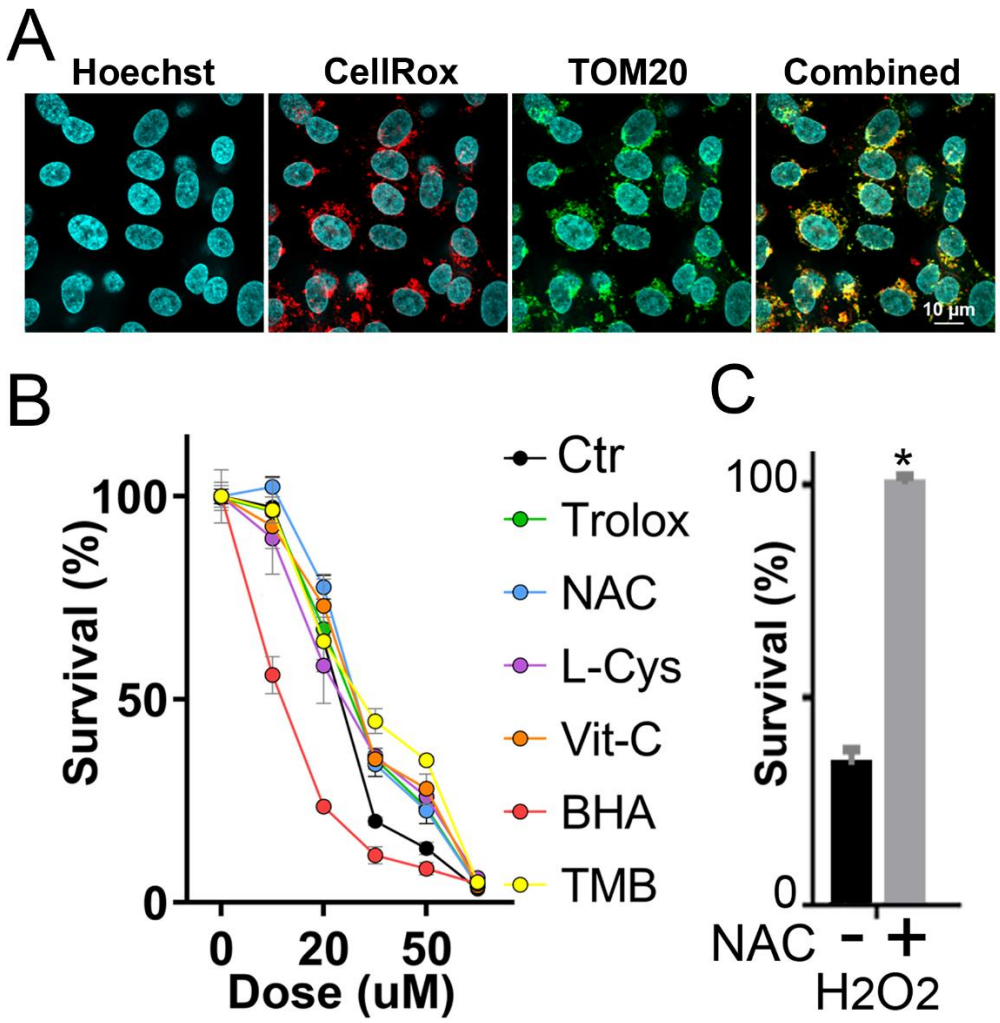

Fig. S5. Light-independent lipofuscin cytotoxicity is not triggered by oxidative-stress. (A) TOM20 (used as a marker for mitochondria) and CellRox (used as probe for ROS) staining on ARPE19 cells showed the colocalization of these two markers. Scale bar is 10 µm. (B) Antioxidants cannot prevent the dose dependent lipofuscin cytotoxicity. ARPE19 cells were pretreated for 1 h with the indicated drugs and then challenged to accumulate A2E for 24 h in the dark. Survival was measured using resazurin fluorescence assay. (B) H_2O_2 oxidative cell-death was prevented with antioxidant (NAC) ($p<0.001$, n=3, mean±SEM, paired t test, GraphPad Prism7.0).

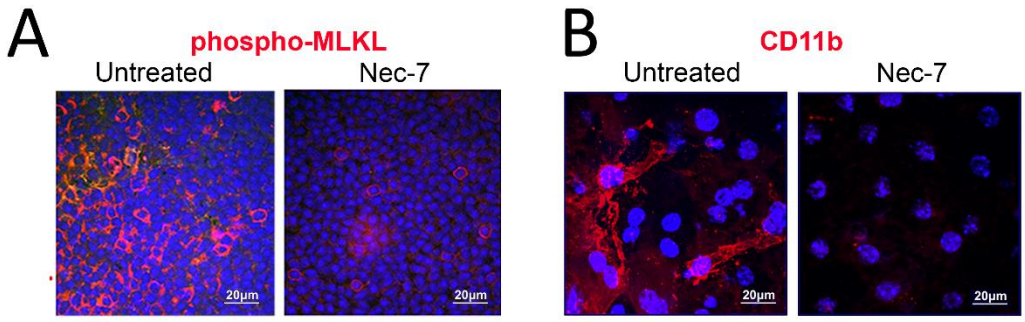

Fig. S6. (A) Representative neuroretina flat mount, showing the reduction of phospho-MLKL in the photoreceptor after receiving intraocular Nec7, one week earlier. (B) Subretinal infiltration of CD11b cells on RPE-flat mounts in 18 to 20-months-old DKOs after receiving mock or Nec7, one week earlier.

TABLE. S1 Chemical inhibitors

Name	Inhibitor of	Company	Cat.no.	Application	Final conc.
Methyl beta Cyclodextrin (MβCD)	Detergent effect	SIGMA	C4555	Cell culture	10 μM
Disulfiran	GasderminD	Cayman Chemical	15303	Cell culture	1-100 uM
Necrosulfonamide (NSA)	MLKL	Cayman Chemical	20844	Cell culture	33 μM
Nec-1	RIPK1	Cayman Chemical	20924	Cell culture	33 μM
Nec-1	RIPK1	Cayman Chemical	11658	Cell culture	33 μM
Nec-2	RIPK1	Cayman Chemical	11657	Cell culture	33 μM
Nec-5	RIPK1	Cayman Chemical	10527	Cell culture	33 μM
Nec-7	Necroptosis	Cayman Chemical	10528	Cell culture	33 μM
TROLOX	Antioxidant	Cayman Chemical	10011659	Cell culture	200 μM
NAC	Antioxidant	SIGMA	A8199	Cell culture	2 mM
L-Cysteine	Antioxidant	SIGMA	C7880	Cell culture	1 mM
L-Ascorbic Acid	Antioxidant	Cayman Chemical	14656	Cell culture	1 mM
H2O2	Pro-oxidant	SIGMA	470226	Cell culture	1 mM
Butylated hydroxyanisole (BHA)	Antioxidant	SIGMA	W218308	Cell culture	1 mM
3,4',5-Trismethoxy Benzophenone (TMB)	Antioxidant	Cayman Chemical	70450	Cell culture	10 μg/ml
ZVad (Q-VD-OPH)	Pan-caspase	Cayman Chemical	15260	Cell culture	1 μM
Deferoxamine (DFO)	Ferroptosis	Cayman Chemical	14595	Cell culture	25-200 μM
GSK'840	RIPK3	AOBIOUS	AOB0917	Cell culture	10 μM
GSK'843	RIPK3	SIGMA	SML2001	Cell culture	10 μM
GSK'872	RIPK3	AOBIOUS	AOB4898	Cell culture	10 μM
LLOMe	Inducer LMP	Cayman Chemical	16008	Cell culture	0.5-2 mM
Arimoclomol	Inhibitor LMP	Medkoo	326988	Cell culture	100 μM

Table S2. Antibodies and Fluorescent probes

					Dilution		
Target	Clone	Company	Cat. No.	Application	WB	IF	cells
CD11b	H5A45	DSHB	H5A45	IF		1:100	
CellRox		ThermoFisher	C10422	ROS probe		1:500	
DRAQ7		Invitrogen	D15106	Necrosis			1:300
Galectin-3	B2C10	BD Sciences	MA140229	IF		1:100	
IBA-1	20A12.1	Millipore	MABN92	IF		1:200	
Lamp1	H4A3	DSHB	H4A3-c	IF		1:100	
Lamp1	1D4B	DSHB	1D4B-c	IF		1:100	
MLKL	D216N	Cell Signaling	14993	WB	1:300		
MLKL	3H1	Millipore	MABC604	IP	1:40		
NucView® 405		Biotium	10405T	Caspase-3 /Apoptosis			1:500
Phalloidin		Biotium	0052	Actin probe		1:50	
p-MLKL	EPR9514	Abcam	Ab187091(H)	IF		1:250	
p-MLKL	EPR9515	Abcam	Ab196436(M)	IF		1:250	
Resazurin 1g/150ml PBS		Sigma	199303	Viability			1:200
Rhodopsin		Abcam	Ab3267	IF		1:200	
TOM20	D8T4N	Cell Signaling	42406	IF		1:100	
ZO-1	1A12	Invitrogen	33-9100	IF		1:100	
β-Actin	13E5	Cell Signaling	4970	WB	1:10,000		

SI References

1. A. Maminishkis, *et al.*, Confluent monolayers of cultured human fetal retinal pigment epithelium exhibit morphology and physiology of native tissue. *Invest. Ophthalmol. Vis. Sci.* **47**, 3612–24 (2006).
2. J. R. Sparrow, C. A. Parish, M. Hashimoto, K. Nakanishi, A2E, a lipofuscin fluorophore, in human retinal pigmented epithelial cells in culture. *Invest. Ophthalmol. Vis. Sci.* **40**, 2988–95 (1999).
3. R. A. Radu, *et al.*, Accelerated accumulation of lipofuscin pigments in the RPE of a mouse model for ABCA4-mediated retinal dystrophies following Vitamin A supplementation. *Invest. Ophthalmol. Vis. Sci.* **49**, 3821–9 (2008).